A PLATINUM-ENRICHED γ+γ′ TWO-PHASE BOND COAT ON NI-BASED SUPERALLOYS

Y. Zhang, Y. Q. Wang, and D. A. Ballard
Department of Mechanical Engineering, Box 5014
Tennessee Technological University, Cookeville, TN 38505-0001
E-mail: yzhang@tntech.edu; Tel.: (931) 372-3265; Fax: (931) 372-6345

B. A. Pint, J. A. Haynes, K. M. Cooley, and I. G. Wright
Metals and Ceramics Division
Oak Ridge National Laboratory, Oak Ridge, TN 37831-6156
E-mail: pintb@ornl.gov; Tel.: (865) 576-2897; Fax: (865) 241-0215

ABSTRACT

A Pt-enriched γ+γ′ two-phase coating was applied to directionally-solidified Ni-based superalloy René 142 substrates with three different Hf levels (0.02, 0.76, and 1.37 wt.%). The coating was prepared by electroplating a thin layer of Pt on the superalloy followed by a diffusion treatment. The as-deposited coating exhibited a γ+γ′ two-phase microstructure with a major composition of Ni-16Al-18Pt-7Cr-9Co (in at.%) along with some incorporation of refractory elements from the substrates. Cyclic oxidation testing at 1100°C in air indicated improved oxidation resistance of the René 142 alloys with the Pt-enriched γ+γ′ coatings. In addition, the oxidation resistance of both uncoated and coated alloys was proportional to the Hf content in the substrate. Compared with the single-phase β-(Ni,Pt)Al coating, slightly higher mass gains and localized spallation were observed on the γ+γ′ two-phase coating, which might be due to the segregation of refractory elements and high sulfur levels in these superalloy substrates.

INTRODUCTION

The constant demand for increased operating temperatures in gas turbine engines has been the driving force for development of more reliable thermal barrier coating (TBC) systems to protect Ni-based superalloys.[1] The single-phase β-(Ni,Pt)Al coating has been an accepted industrial standard as the bond coat for TBCs deposited by electron beam-physical vapor deposition (EB-PVD), which can be fabricated by electroplating the superalloy with a layer of Pt followed by an aluminizing process such as chemical vapor deposition (CVD).[2] Failure of EB-PVD TBCs is often associated with spallation of the Al_2O_3 scale along the scale-bond coat interface and/or deformation of the bond coat surface.[3] In engine service, due to formation of the Al_2O_3 scale and interdiffusion with the superalloy, depletion of Al leads to phase transformations from the as-deposited β-(Ni,Pt)Al to the martensite and γ′-Ni_3Al.[4-6] The new phases possess different creep and/or yield strengths which could affect the ability of the bond coat to accommodate the Al_2O_3 scale. Volume changes associated with these phase transformations could also contribute to rumpling at the bond coat surface.[7,8] Furthermore, for newer-generation superalloys with higher Re content, formation of secondary reaction zone underneath the (Ni,Pt)Al coating is detrimental to mechanical integrity of the TBC system.[9]

A recent study by Gleeson et al. has indicated that the cast alloy Ni-22Al-30Pt+Hf (at.%) with a γ+γ′ microstructure can form an adherent α-Al_2O_3 scale with significantly reduced rumpling during thermal cycling.[10] Also, initial work in Europe has indicated promising coating performance for a Pt-enriched γ+γ′ bond coat.[11] The γ+γ′ coating can be synthesized by electroplating a 5-10μm of Pt followed by a diffusion treatment.[12] It is believed that the γ+γ′ coating could offer potential advantages over the β-(Ni,Pt)Al coating, such as higher creep strength (thus more resistant to mechanical damage),

better compatibility between coating and superalloy substrate, and reduced fabrication cost with eliminating the aluminizing process.[13] Despite the potentials of the γ+γ'-type bond coat, very little is known with regard to its oxidation performance.[14] In this study, the oxidation behavior of Pt-enriched γ+γ' coatings on René 142 Ni-based superalloy was investigated, and compared with the β-(Ni,Pt)Al coating. The effect of alloying elements in the superalloy substrates on the coating oxidation behavior was examined.

EXPERIMENTAL PROCEDURES

Directionally-solidified (DS) Ni-based superalloy René 142 substrates with three Hf levels were coated. The nominal alloy composition was Ni-6.0Al-6.7Cr-11.8Co-6.3Ta-4.8W-1.5Mo-2.8Re-0.01Ti, in wt.% (Ni-13.3Al-7.7Cr-12.0Co-2.1Ta-1.6W-0.94Mo-0.90Re-0.01Ti, in at.%), and the alloys, designated as A, B, and C, contained 0.02, 0.76, and 1.37 wt.% of Hf, respectively. All of the alloys contained ~20 ppmw sulfur which was somewhat higher than commercial René 142 (~6 ppmw).[15] The Pt-enriched γ+γ' two-phase coating was prepared by electroplating ~7μm Pt on the superalloy followed by a diffusion treatment for 2h in vacuum (~1.3 x 10^{-5} Pa) at 1150°C. Prior to Pt plating, the substrate was grit-blasted using #220 Al_2O_3 grit and ultrasonically cleaned in acetone. Cyclic oxidation tests with 1h cycles were conducted on the coated and uncoated specimens at 1100°C in air. For comparison, the β-(Ni,Pt)Al coating on René 142-C fabricated in a laboratory CVD reactor was included.[16] Selected specimens were examined by field emission gun-scanning electron microscopy (FEG-SEM) equipped with energy dispersive spectroscopy (EDS) and electron probe microanalysis (EPMA).

RESULTS AND DISCUSSION

Figure 1 shows a cross-sectional image of the Pt-enriched γ+γ' coating on René 142-A (0.02 Hf) and the compositional profiles measured by EPMA. The coating was ~30μm thick with two distinct phases; the lighter phase was Pt-enriched γ' and the darker phase was Pt-enriched γ, as illustrated in Fig. 1(a).[17] The average composition in the γ+γ' coating was Ni-16Al-18Pt-7Cr-9Co, in at.% (Ni-5Al-43Pt-4Cr-6Co, in wt.%), as shown in Fig. 1(b). The Pt concentration was substantially higher than that in CVD β-(Ni,Pt)Al coating, which is typically ~5 at.% (or 20 wt.%).[16] There was significant incorporation of refractory elements, e.g., Ta-1.7 at.% (3.9 wt.%), W-1.0 at.% (2.2 wt.%), Mo-0.7 at.% (0.8 wt.%), and Re-0.5 at.% (1.2 wt.%).

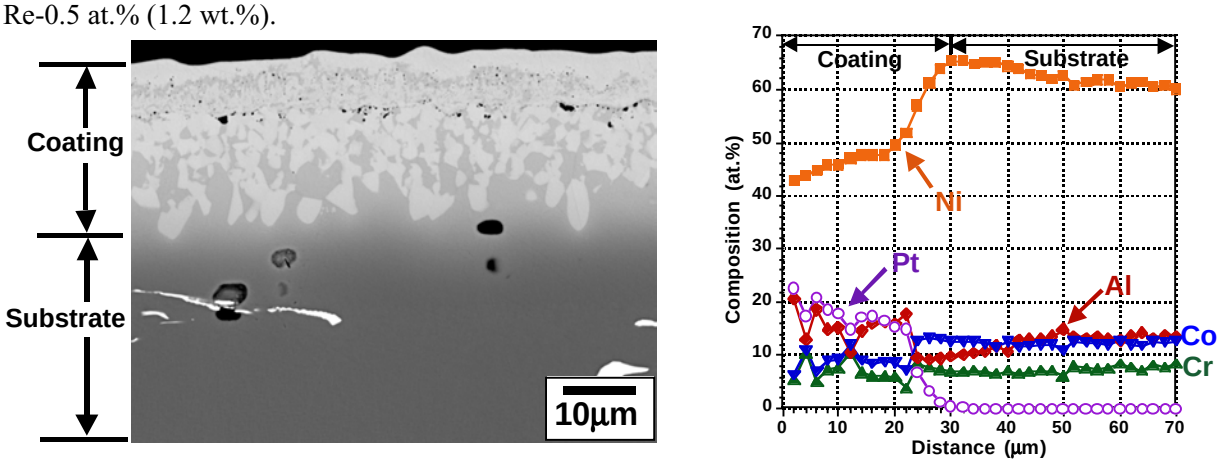

(a) (b)

Figure 1. (a) Back-scattered electron image of cross section of an as-deposited γ+γ' coating on René 142-A, and (b) compositional profiles of the major elements measured by EPMA.

The mass changes of the coated and uncoated alloys during cyclic oxidation at 1100°C are compared in Fig. 2. Without a coating, all three alloys registered continuous mass loss during cycling, Fig. 2(a). The B and C alloys had noticeably better performance than the A alloy; the C alloy, with the highest Hf level (1.37 wt.%), showed the best performance. A study by Ross and O'Hara [19] indicated that commercial René 142 performed better than second-generation single-crystal alloys CMSX-4 and PWA 1484 during a burner rig oxidation test at 1176°C (2150°F). It should be noted that the present alloys contained higher S than the commercial alloys. Compared to the bare alloys, the oxidation performance of γ+γ′-coated René 142 was drastically improved. The mass change data was replotted over a smaller ordinate range in Fig. 2(b). After 300 cycles, significant oxide spallation occurred on the coated A and B alloys with lower Hf contents, so the test was terminated on these alloys and the coatings were sectioned (a coated C alloy specimen, Pt/Alloy C1, also was pulled out of the furnace for comparison). A second C alloy specimen with the γ+γ′ coating (Pt/Alloy C2) was tested for 800 cycles. A relatively small mass gain was measured after 700 cycles, although it was higher than the β-(Ni,Pt)Al coating, Fig. 2(b).

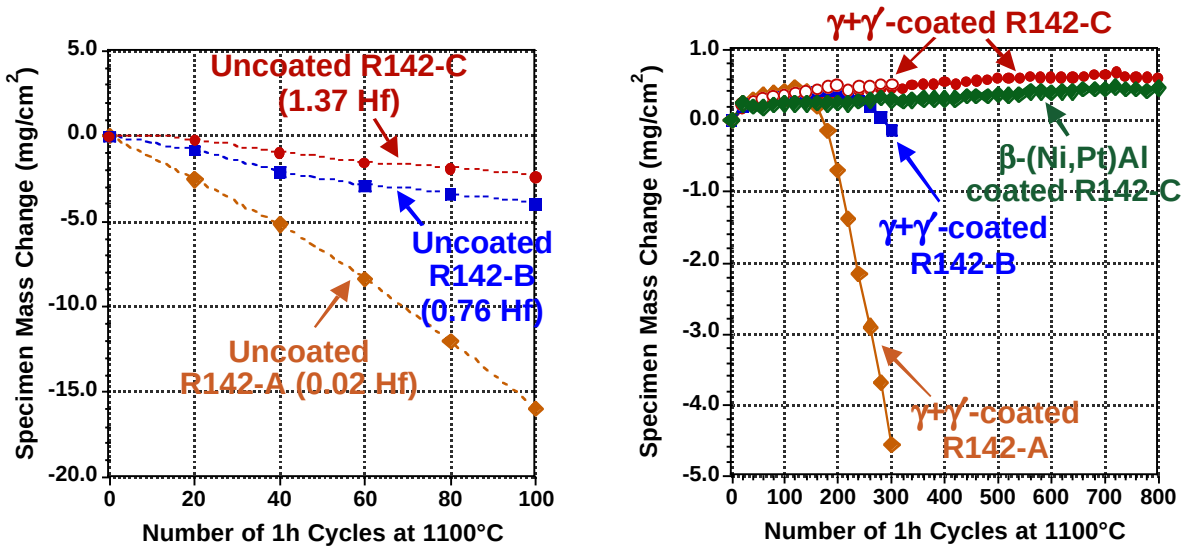

(a) (b)

Figure 2. Specific mass change during 1h cyclic oxidation testing at 1100°C: (a) uncoated and γ+γ′-coated alloys, and (b) γ+γ′- and (Ni,Pt)Al-coated specimens. Note the difference in the scale range of (a) and (b).

Analysis of the oxidized coating surfaces by SEM revealed significant spallation of oxide scales on the coated A and B alloys after 300 cycles, as shown in Figs. 3(a) and (b), while the majority of the alumina scale was intact on the coated C alloy with either two-phase γ+γ′ or single-phase β-(Ni,Pt)Al coating, as depicted in Figs. 3(c) and (d). Minor cracking was noticed on the β-(Ni,Pt)Al coating, as indicated by the arrows in Fig. 3(d).

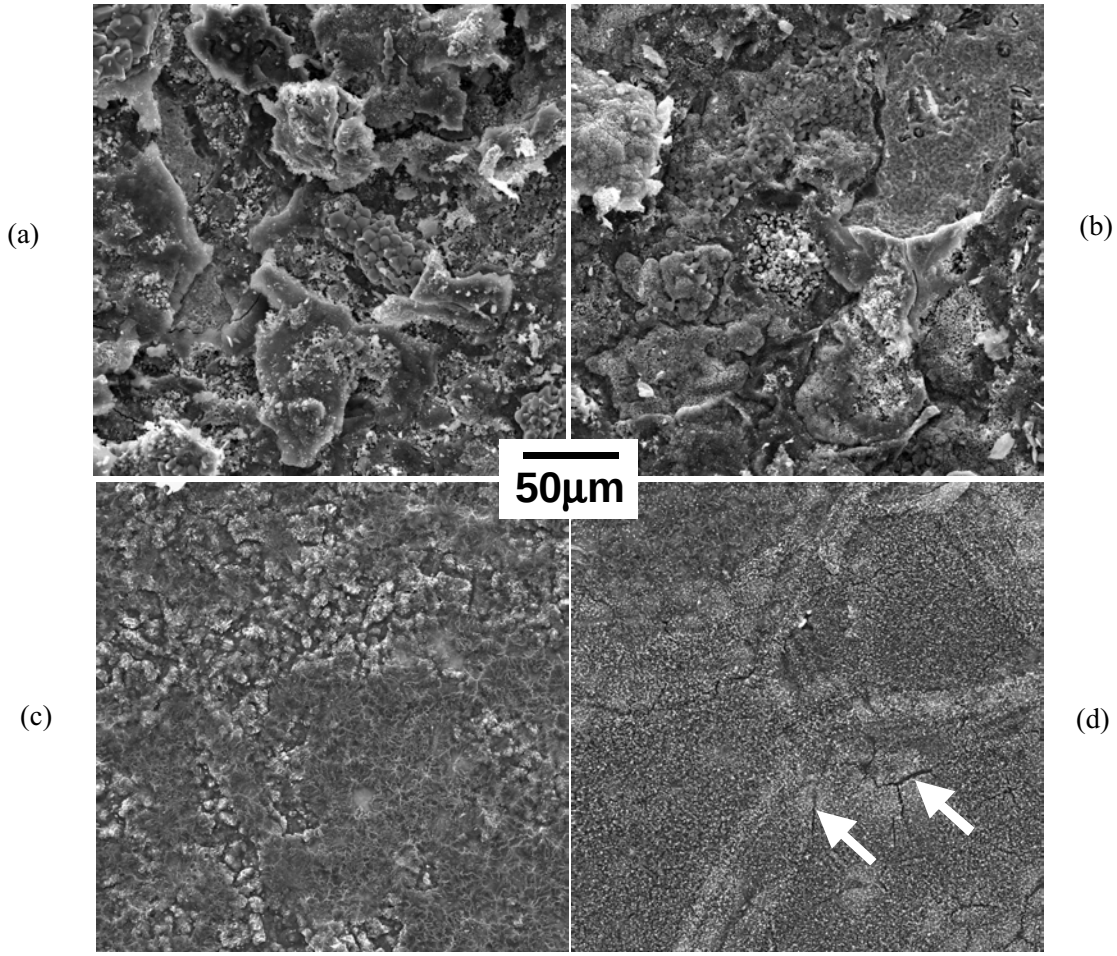

Figure 3. Secondary-electron images of surface morphology of coated René 142 after 300 1h cycles at 1100°C: (a), (b) and (c) γ+γ′-coated A, B, C alloys, respectively; (d) β-(Ni,Pt)Al-coated C alloy, where the arrows point to the minor cracks in the scale.

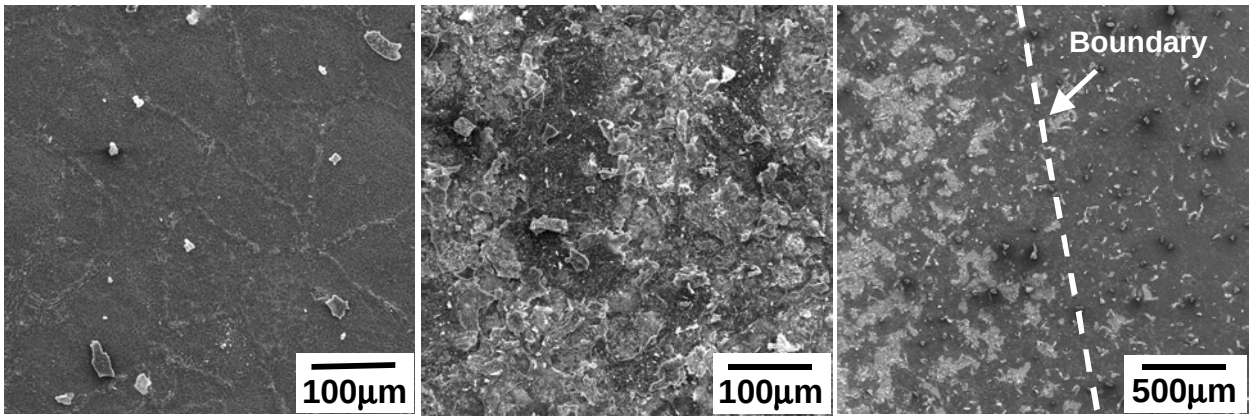

Figure 4. Secondary-electron images of surface morphology of γ+γ′-coated René 142-C after 800 1h cycles at 1100°C: (a) and (b) "good" and "bad" regions, respectively; (c) the boundary between these two regions.

After 800 cycles, a uniform and adherent scale remained on the C alloy with the β-(Ni,Pt)Al coating. Adherent scales formed on most surface area of the γ+γ'-coated René 142-C, Fig. 4(a). However, spallation occurred at certain locations (near the specimen center), as shown in Fig. 4(b). Ni-rich oxides and Hf-rich precipitates were observed in the spallation area. More interestingly, a clear boundary existed between the adherent and non-adherent scales, as illustrated by the dashed line in Fig. 4(c). This regional difference in oxidation behavior also was noticed on the cross section of the γ+γ'-coated René 142-C after 300 cycles. A thin adherent Al_2O_3 scale was found in the region shown in Fig 5(a), whereas thicker internal oxides rich in Hf and other alloying elements were observed in another region, Fig. 5 (b).

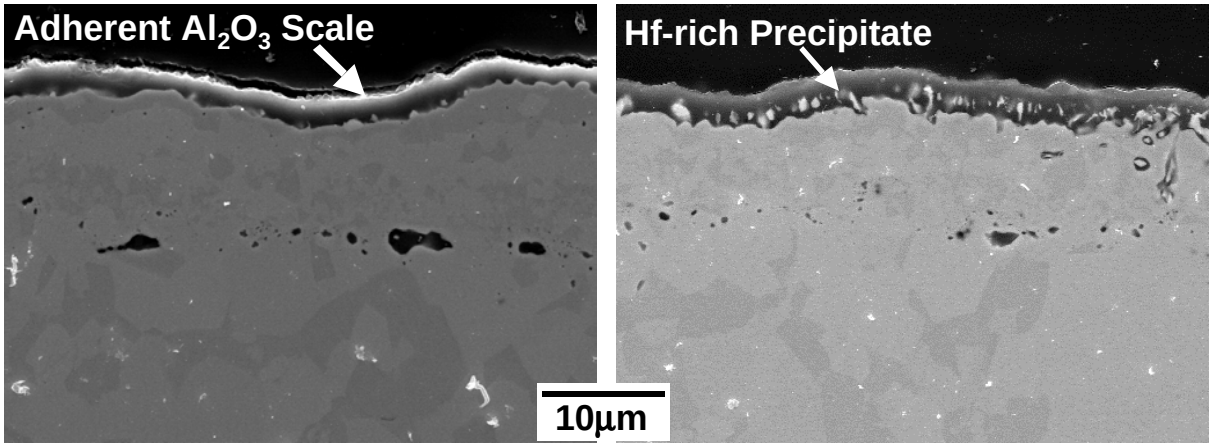

(a) (b)

Figure 5. Secondary-electron images of cross section of γ+γ' coating on René 142-C after 300 1h cycles at 1100°C: (a) the "good" region with a thin and adherent scale, and (b) the "bad" region with precipitates rich in Hf and other alloying elements in the scale.

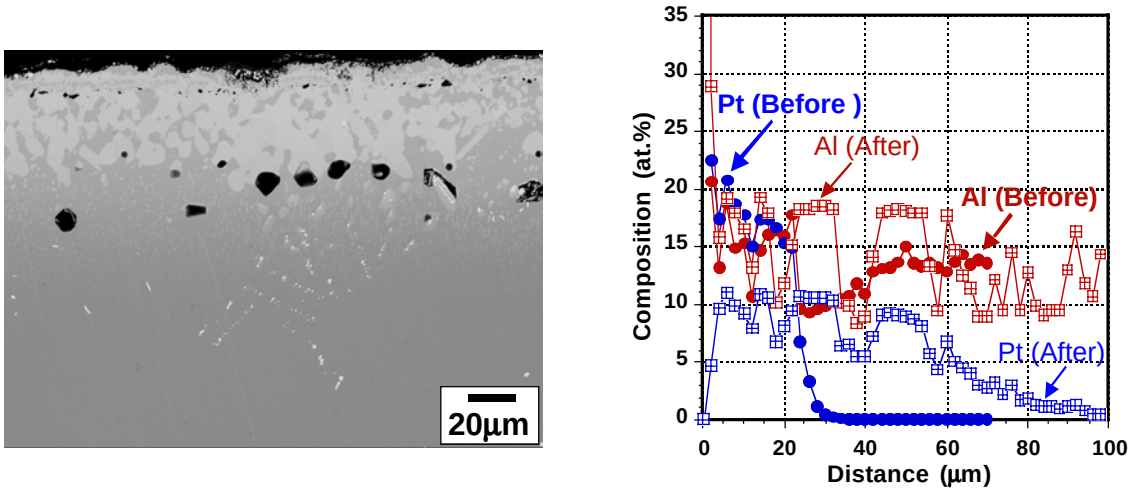

(a) (b)

Figure 6. (a) Back-scattered electron image of cross section of γ+γ' coating on René 142-C after 300 1h cycles at 1100°C, and (b) comparison of the compositional profiles of Al and Pt before and after 300 1h cycles at 1100°C.

Figure 6 depicts a cross section and compositional profiles of the γ+γ' coating on René 142-C after 300 1h cycles at 1100°C. While the two-phase structure was maintained in the coating, the γ' phase

became more agglomerated, as shown in Fig. 6(a). After 300h at 1100°C, the Al level remained nearly unchanged in the coating, ~15 at.%, whereas Pt decreased from ~18 to ~8 at.% and it diffused into the substrate to a depth of ~95 μm, as illustrated in Fig. 6(b). The contents of other alloying elements such as Cr, Co and refractory elements (which are not shown in the figure) did not change significantly.

These results indicate promising oxidation performance of the Pt-enriched γ+γ′ coating at 1100°C. The beneficial effect of Hf in the substrate alloy on γ+γ′ coating oxidation resistance was evident. The oxidation resistance of the coating was proportional to the Hf content in the superalloy (0.02 to 1.37 wt.% Hf). However, the oxide scales formed on the present γ+γ′ coating were not as adherent as compared to the β-(Ni,Pt)Al bond coat. Localized spallation was found after 800 cycles on the γ+γ′-coated René 142-C. The segregation of refractory elements in the substrate alloy might contribute to such regional difference in scale adhesion of the γ+γ′ coating. As indicated by the cross section of the as-deposited coating in Fig. 7, a boundary could be seen between a nearly clean region in the cast substrate and a region with more segregation of refractory elements. More detailed characterization will be needed to clarify any connections between the chemical segregation in the superalloy substrate and scale spallation of the γ+γ′ coating during thermal cycling.

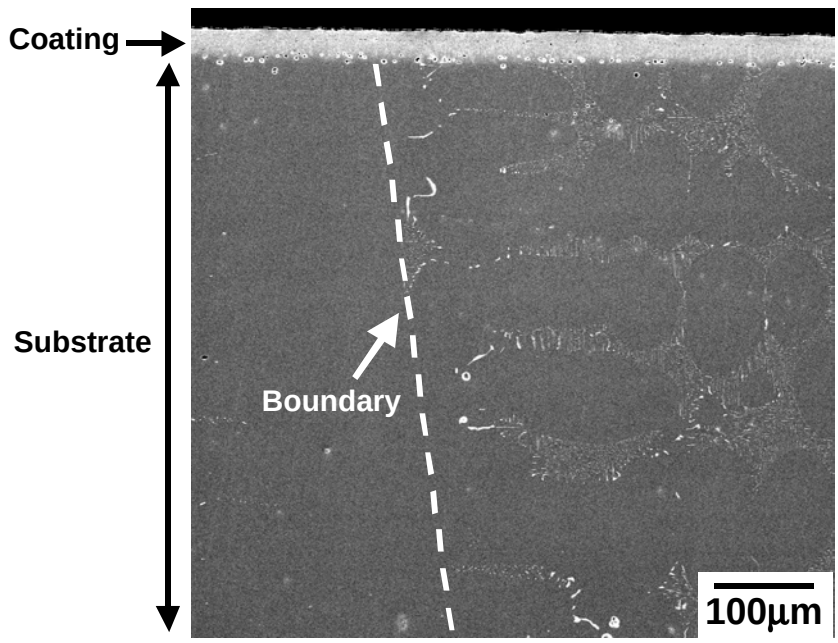

Figure 7. Secondary-electron image of etched cross section of as-deposited γ+γ′ coating indicating the segregation in the cast superalloy.

Depending on the superalloy composition, alloying elements such as Cr, Co, Ta, W, Re, Ti, Mo and Hf become incorporated into the Pt-enriched γ+γ′ coating, in contrast to the cast Ni-Al-Pt+Hf alloys in Gleeson's study.[10] The composition of substrate alloys could have a more profound effect on oxidation performance of the γ+γ′-type bond coat than the β-(Ni,Pt)Al due to higher solubility of refractory metals in the γ and γ′ phases. Significant difference in TBC lifetime has been reported for the Pt-enriched γ+γ′ bond coat on two single-crystal alloys, CMSX-4 and RR-3000. The coated RR-3000 exhibits ~10x lifetime over CMSX-4.[17] Also, sulfur impurities, from both substrates and Pt electroplating process, could have detrimental effect on oxidation resistance of the γ+γ′ coatings,[19, 20] The René 142 alloys used in the present study contained relatively high S content, ~20 ppmw, which could have adversely affected the coating oxidation behavior. An initial study on the oxidation

performance of low-sulfur single-crystal René N5 at 1150°C with the γ+γ' coatings indicated improved oxidation resistance over the coating on René 142-C, as shown by the mass changes in Fig. 8. The γ+γ' coating on René N5 which contained 0.4 ppmw S showed less spallation than on René 142-C with ~20 ppmw S. Also, it is worth to point out that the γ+γ' coating fabricated by a laboratory Pt plating process exhibited better oxidation behavior than commercial Pt plating, which was due to less contamination such as S during Pt plating. However, in general, the oxidation resistance of the current γ+γ' coating was inferior to the single-phase β-(Ni,Pt)Al coating.

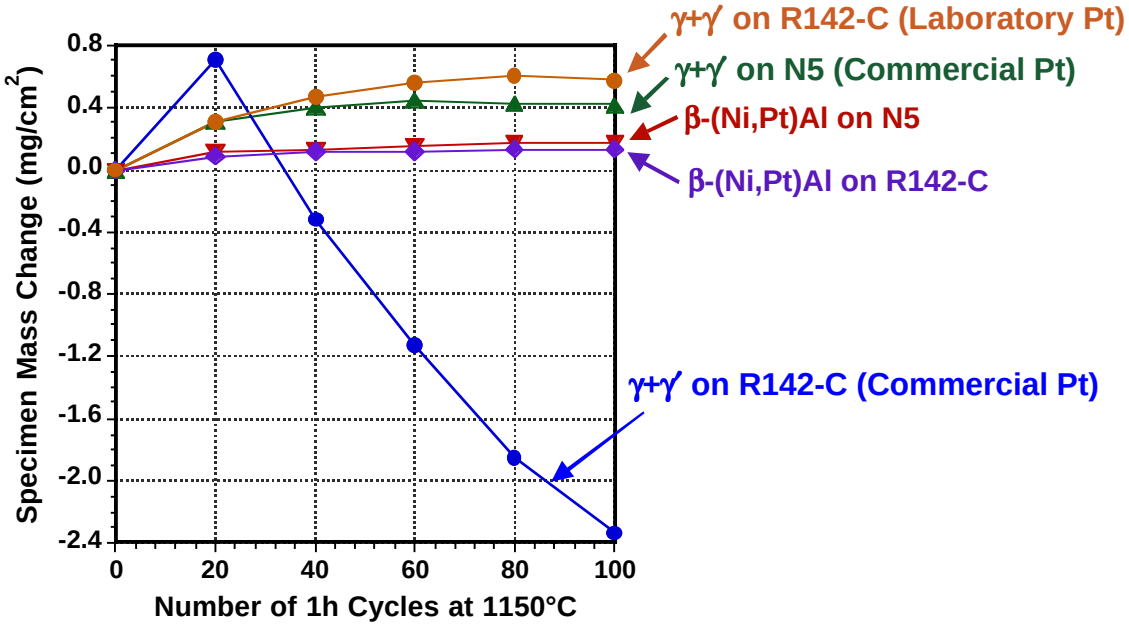

Figure 8. Specific mass change during 1h cyclic oxidation testing at 1150°C of coated René N5 and René 142-C alloys.

CONCLUSIONS

A Pt-enriched γ+γ' two-phase coating was applied to the DS René 142 Ni-based superalloy by electroplating ~7μm Pt followed by a diffusion treatment for 2h in vacuum at 1150°C. Compared to bare alloys, the γ+γ' coating on René 142 alloys showed improved cyclic oxidation resistance at 1100°C, especially for the alloys with higher Hf levels. However, compared with the β-(Ni,Pt)Al coating, the present γ+γ' coating showed slightly higher mass gains and localized spallation, which might relate to segregation of refractory metals and high S levels in these superalloy substrates.

ACKNOWLEDGEMENTS

The authors acknowledge K. M. Cooley, G. W. Garner, L. D. Chitwood, K. S. Reeves, and L. R. Walker at Oak Ridge National Laboratory (ORNL) for assisting with the experimental work, and P. F. Tortorelli at ORNL for reviewing the manuscript. This research was sponsored by the U.S. Department of Energy, Fossil Energy Advanced Materials Research Program, under contract DE-AC05-00OR22725 with UT-Battelle LLC and subcontract 4000032193 with Tennessee Technological University.

REFERENCES

1. G. W. Goward, *Surf. Coat. Technol.*, 108-109 (1998) 73.
2. B. M. Warnes and D. C. Punola, *Surf. Coat. Technol.*, 94-95 (1997) 1.
3. S. M. Meier, D. M. Nissley, K. D. Sheffler, and T. A. Cruse, *J. Eng. Gas Turb. Power*, 114 (1992) 258.
4. Y. Zhang, J. A. Haynes, B. A. Pint, I. G. Wright, and W. Y. Lee, *Surf. Coat. Technol.*, 163-164 (2003) 19.
5. M. W. Chen, R. T. Ott, T. C. Hufnagel, P. K. Wright, and K. J. Hemker, *Surf. Coat. Technol.*, 163-164 (2003) 25.
6. S. Darzens, D. R. Mumm, D. R. Clarke, and A. G. Evans, *Metall. Mater. Trans.*, 34A (2003) 511.
7. V. K. Tolpygo and D. R. Clarke, *Acta Mater.*, 48 (2000) 3283.
8. D. R. Mumm, A. G. Evans, and I. T. Spitsberg, *Acta Mater.*, 49 (2001) 2329.
9. S. Walston, in *Superalloys 2004*, K. A. Green, T. M. Pollock, H. Harada, T. E. Howson, R. C. Reed, J. J. Schirra, and S, Walston, eds. (TMS, 2004), pp. 579.
10. B. Gleeson, W. Wang, S. Hayashi, and D. Sordelet, *Mater. Sci. Forum*, 461-464 (2004) 213.
11. J. R. Nicholls, *MRS Bulletin*, Sept. (2003) 659.
12. D. S. Rickerby, S. R. Bell, and R. G. Wing, *US Patent* No. 5,667,663, 1997.
13. B. A. Nagaraj, W. B. Connor, R. W. Jendrix, D. J. Wortman, and L. W. Plemmons, *US Patent* No. 5,427,866, 1995.
14. O. A. Adesanya, K. Bouhanek, F. H. Stott, P. Skeldon, D. G. Lees, and G. C. Wood, *Mater. Sci. Forum*, 369-372 (2001) 639.
15. J. L. Smialek, *Oxid. Met.*, 55 (2001) 75.
16. Y. Zhang, W. Y. Lee, J. A. Haynes, I. G. Wright, B. A. Pint, K. M. Cooley and P. K. Liaw, *Metall. Mater. Trans.*, 30A (1999) 2679.
17. K. Bouhanek, O. A. Adesanya, F. H. Stott, P. Skeldon, D. G. Lees, and G. C. Wood, *Mater. Sci. Forum*, 369-372 (2001) 615.
18. E. W. Ross and K. S. O'Hara, in *Superalloys 1992*, S. D. Antolovich, R. W. Stusrud, R. A. MacKay, D. L. Anton, T. Khan, R. D. Kissinger, and D. L. Klarstrom, eds. (TMS, 1992), pp. 257.
19. J. L. Smialek, D. T. Jayne, J. C. Schaeffer, and W. H. Murphy, *Thin Solid Films*, 253 (1994) 285.
20. B. A. Pint, I. G. Wright, W. Y. Lee, Y. Zhang, K. Prüβner, and K. B. Alexander, *Mater. Sci. Eng.*, A245 (1998) 201.